Prediction of Remaining Useful Life of Lithium-ion Battery based on Multi-kernel Support Vector Machine with Particle Swarm Optimization

Dong Gao[*] and Miaohua Huang[†]

[*],[†]Hubei Key Laboratory of Advanced Technology for Automotive Components,
Wuhan University of Technology, Wuhan, China

Abstract

The estimation of the remaining useful life (RUL) of lithium-ion (Li-ion) batteries is important for intelligent battery management system (BMS). Data mining technology is becoming increasingly mature, and the RUL estimation of Li-ion batteries based on data-driven prognostics is more accurate with the arrival of the era of big data. However, the support vector machine (SVM), which is applied to predict the RUL of Li-ion batteries, uses the traditional single-radial basis kernel function. This type of classifier has weak generalization ability, and it easily shows the problem of data migration, which results in inaccurate prediction of the RUL of Li-ion batteries. In this study, a novel multi-kernel SVM (MSVM) based on polynomial kernel and radial basis kernel function is proposed. Moreover, the particle swarm optimization algorithm is used to search the kernel parameters, penalty factor, and weight coefficient of the MSVM model. Finally, this paper utilizes the NASA battery dataset to form the observed data sequence for regression prediction. Results show that the improved algorithm not only has better prediction accuracy and stronger generalization ability but also decreases training time and computational complexity.

Key words: Lithium-ion battery RUL, Multi-kernel support vector machine, Particle swarm optimization algorithm, RUL prediction

I. INTRODUCTION

Environmental issues triggered by emissions from conventional vehicles have accelerated the adaptation of electric vehicles (EVs) for urban transportation [1]. Lithium-ion (Li-ion) batteries have been widely used in many new energy systems as a power source because of their high-energy density, long service life, and low pollution. Li-ion batteries are used as the energy source for many devices. Thus, they are quickly becoming the most common power source for EVs [2]. Remaining useful life (RUL) is the useful life left on the Li-ion battery at a particular time of operation. The estimation of the RUL of Li-ion batteries is essential to prognostics and health management (PHM) [3].

The batteries are subjected to physical and chemical degradation during their operations. The main factors of degradation are related to electrode corrosion and electrolyte degradation. Some methods have been developed to estimate and calculate the state of health (SOH) of battery [4]-[6].

In recent years, many studies on the degradation model and the RUL prediction of Li-ion batteries have been conducted. Various techniques and methods are proposed to improve the prediction accuracy of the RUL of Li-ion battery. These techniques and methods can be divided into two categories, namely, model-based prognostics and data-driven prognostics.

Model-based prognostics require a deep understanding of the composition of the model, in which mathematical expressions are used to describe the complex electrochemical process. Moreover, the explicit analysis of the solutions is difficult because the model is always non-linear. Lumped-element equivalent-circuit components, such as resistors and capacitors, are used to represent the behavior of a battery cell [7]. Many studies have used Kalman filtering

with electrochemical or electrical equivalent-circuit models for monitoring, e.g., Refs. [8], [9]. With the development of measurement technology and reduced cost, electrochemical impedance spectroscopy (EIS), a non-invasive method, has been used to characterize battery capacity degradation through variations of internal parameters [10]. Ref. [11] presents a method based on the internal resistance growth model using the particle filtering (PF) approach to estimate the RUL of Li-ion batteries. A model-based Bayesian approach is proposed in Ref. [12] to predict the RUL for these types of batteries.

Data-driven prognostics consider Li-ion battery as a black box without figuring out the complex electrochemical process in the model. Thus, the only mathematical laws of the historical data of the Li-ion battery should be determined to predict its capacity or RUL. Algorithms or related parameters are the main factors that affect the accuracy of RUL prediction.

Data-driven prognostics do not need to study the battery model directly because all information about Li-ion batteries, which is obtained through data analysis, has been fully reflected in the collected data. Data-driven prognostics can obtain implicit information between the input and output through training samples and finally forecast the future trend. In the background of big data analysis, data-driven prognostics have a good value for the RUL prediction of Li-ion batteries.

With the rapid development of machine-learning technology and artificial intelligence (AI), more algorithms are used to predict the RUL of Li-ion batteries. For example, a data-driven approach using an improved auto regressive (AR) model by particle swarm optimization (PSO) for the RUL prediction of Li-ion batteries is proposed in Ref. [13]. A data-driven approach that combines empirical mode decomposition (EMD) and AR integrated moving average (ARIMA) model for RUL prognostic is proposed in Ref. [14]. In Ref. [15], a data-driven method is developed using the unscented Kalman filter (UKF) with relevance vector regression (RVR), which is used for RUL and short-term capacity prediction of batteries. An intelligent prognostic for battery health based on the sample entropy feature of discharge voltage is proposed in Ref. [16]. Similarly, particle filter (PF) was used to predict RUL and time until the end of the discharge voltage of the Li-ion battery in Ref. [17]. In Ref. [18], a multistep-ahead prediction model based on the mean entropy and relevance vector machine (RVM) is developed and applied for SOH and RUL prediction of Li-ion battery. An optimized RVM algorithm is used to improve the accuracy and stability of RUL estimation in Ref. [19]. In Ref. [20], a method that integrates classification and regression attributes of support vector (SV)-based machine-learning technique for real-time RUL estimation of Li-ion batteries is proposed. A method that estimates the SOH of Li-ion battery using health condition parameters by support vector regression-particle filter (SVR-PF), which has provided a good foundation for multi-step ahead prediction, was proposed in Ref. [21]. An online approach using feed-forward neural network (FFNN) and importance sampling (IS) to estimate the RUL of Li-ion battery is presented in Ref. [22]. In Ref. [23], a novel RUL prediction method based on the Gaussian process mixture (GPM), which can process multimodality by fitting different segments of trajectories with different Gaussian process regression (GPR) models separately, such that the tiny differences among these segments can be revealed, is proposed. In Ref. [24], a novel PF-based method for the RUL estimation of Li-ion batteries is developed by combining Kalman filter and PSO. An improved unscented particle filter (IUPF) method, which uses the MCMC to solve the problem of sample impoverishment in unscented particle filter (UPF) algorithm for the RUL prediction of Li-ion battery, is proposed in Ref. [25]. A new data-driven prognostic method based on the interacting multiple model particle filter (IMMPF) to determine the RUL of Li-ion batteries and the probability distribution function (PDF) of the associated uncertainty is proposed in Ref. [26].

SVM is one of the most powerful and popular machine-learning algorithms used to estimate SOH and RUL. SVM is combined with a completely new method for data processing [27] that can handle non-linear systems and outperform ordinary regression because of its insensitivity to small changes. Besides, the performance of SVM does not directly depend on the dimension of classified entities [28].

SVM is popular in many fields, such as financial time series and power load forecasting. The selection and construction of kernel functions, which have significant influence on the efficiency and generalization performance of the RUL prediction of Li-ion batteries, is crucial when SVM is used to predict the RUL of Li-ion batteries. Moreover, the process of training sample selection will affect the quality of the RUL prediction of Li-ion batteries. The existing kernel function for Li-ion batteries RUL prediction based on SVM is the single kernel function. Refs. [18], [29], [30] all used a single kernel function without considering its limitations. Under certain conditions, the single kernel function shows some learning and generalization capability. However, the construction of kernel function and the selection of related parameters have not been well set up. Several basic forms of kernel functions are often used with different mapping properties, which show significant performance differences in various applications. Using a single kernel function is not reasonable when SVM is used to predict the RUL of Li-ion batteries. Thus, this study introduces a novel multi-kernel SVM with PSO (PSO–MSVM) algorithm to solve the limitations of SVM when applied in the RUL prediction of Li-ion batteries and to improve the accuracy of the prediction.

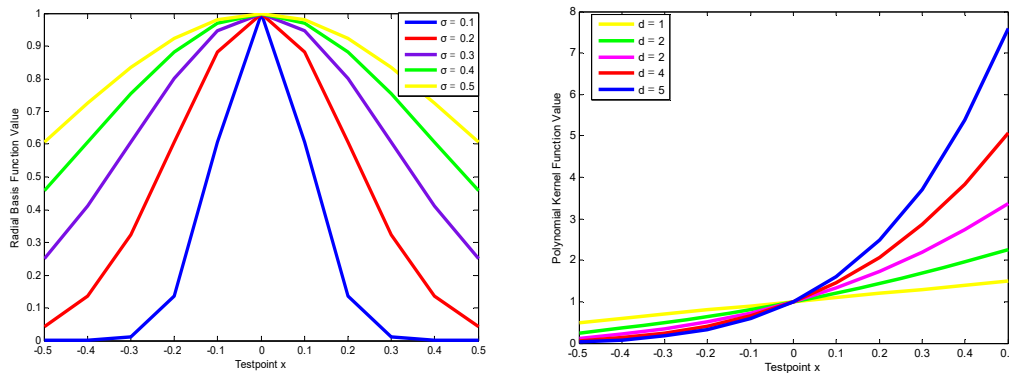In this contribution, data-driven methods are used to

Fig. 1. Curves of different test points for RBF and Polynomial kernel.

predict the RUL of Li-ion batteries using PSO–MSVM, which not only improves the accuracy of prediction but also decreases training time and computational complexity. The rest of this article is organized as follows. Section II introduces the concept of SVM and MSVM algorithm. Section III proposes a practical optimized method to conduct the global optimal search on the key parameters, and further improves the prediction accuracy and calculation speed of the MSVM model. Section IV verifies the PSO–MSVM algorithm based on the NASA battery dataset and analyzes the prediction results. Finally, Section V summarizes the paper.

II. MULTI-KERNEL SVM LEARNING ALGORITHM

A. Support Vector Machine (SVM)

This section introduces some basic theories of SVM. SVM aims to establish an optimal separating hyper-plane as the decision plane by maximizing the distance between positive and negative examples [31], [32].

Given a training dataset $Q = \left\{\mathbf{x}_j, y_j\right\}_{j=1}^n$, $(\mathbf{x}_j \in \mathrm{R}^n, y_j \in \mathrm{R})$, $\mathbf{x}_j$ is the j-th input feature vector, y_j is the class label of $\mathbf{x}_j$, and n is the number of all samples.

When the training sample is completed, an optimal hyper-plane can be established as follows:

$$p(\mathbf{x}) = \mathbf{w}^T \cdot \phi(\mathbf{x}) + b, \qquad (1)$$

where the function of $\phi(\mathbf{x})$ is used to map the input feature vector into high-dimensional feature space, b is a bias term, $\mathbf{w}$ is a vector of the hyper-plane. The estimated values of b and $\mathbf{w}$ can be obtained by solving the following quadratic programs:

$$\min \ T(\mathbf{w}, b, \varepsilon) = \frac{1}{2}\|\mathbf{w}\|^2 + C \sum_{j=1}^n \varepsilon_j, \qquad (2)$$

$$s.t. \ y_j\left(\mathbf{w}^T \cdot \phi(\mathbf{x}_j) + b\right) \geq 1 - \varepsilon_j \quad j = 1, \dots, n, \quad (3)$$

and

$$\varepsilon_j \geq 0 \quad j = 1, \dots, n. \qquad (4)$$

The Lagrangian of the quadratic program in (2)–(4) is

$$L(\mathbf{w}, \varepsilon, b; \boldsymbol{\alpha}) = T(\mathbf{w}, \varepsilon, b) - \sum_{j=1}^n \alpha_j \{y_j(\mathbf{w}^T \cdot$$
$$\phi(\mathbf{x}_j) + b) + \varepsilon_j - 1\} - \sum_{j=1}^n \mu_j \varepsilon_j. \qquad (5)$$

Taking partial derivatives of $L(\mathbf{w}, \varepsilon, b; \boldsymbol{\alpha})$ with respect to the primal variables and substituting the results into $L(\mathbf{w}, \varepsilon, b; \boldsymbol{\alpha})$ in (5) results in the dual formulation of the SVM:

$$\max \ L(\mathbf{w}, \varepsilon, b; \boldsymbol{\alpha}) =$$
$$\left\{\sum_{j=1}^n \alpha_j - \frac{1}{2}\sum_{i,j=1}^n \alpha_i \alpha_j y_i y_j K(\mathbf{x}_i, \mathbf{x}_j)\right\}, \qquad (6)$$

$$s.t. \ \sum_{j=1}^n y_j \alpha_j = 0, \qquad (7)$$

and

$$0 \leq \alpha_j \leq C \quad j = 1, \dots, n, \qquad (8)$$

where α_j is the Lagrange multiplier of observation j, and the inner product function $K(\mathbf{x}_i, \mathbf{x}_j)$ is called the kernel function. High-dimensional feature space in the inner product can implicitly operate by introducing the kernel function of the original space.

The computation of SVM can be simplified by transferring the problem with the Kuhn–Tucker condition into the equivalent Lagrange dual problem. Therefore, the linear decision function is obtained by solving the dual optimization problem, and the SVM problem can be simplified as follows:

$$p(\mathbf{x}) = \mathrm{sgn}\left(\sum_{j=1}^n \alpha_j y_j K(\mathbf{x}_j, \mathbf{x}) + b\right). \qquad (9)$$

The SVM is widely used not only in classification problems but also in regression problems, which are difficult classification problems in essence. SVM has many advantages, such as good robustness, simple calculation, wide universality, and perfect theory.

B. Multi-Kernel SVM Learning Algorithm

The selection of the kernel function of the model is very important when SVM is used to predict the RUL of Li-ion battery. The use of SVM with different kernel functions will form different prediction models, which will produce different prediction accuracies and efficiencies.

The two types of kernel functions commonly used in SVM are global kernel and local kernel.

Radial basis function (RBF) kernel is a typical local kernel. Its mathematical form is defined as follows [33]:

$$K_{RBF}(\mathbf{x}_i, \mathbf{x}_j) = \exp\left(-\frac{1}{2\sigma^2}\|\mathbf{x}_i - \mathbf{x}_j\|^2\right), \qquad (10)$$

where σ is the parameter of the kernel.

Polynomial kernel is a typical global kernel, which is defined as follows [34]:

$$K_{poly}(\mathbf{x}_i, \mathbf{x}_j) = (\mathbf{x}_i^T \mathbf{x}_j + 1)^d, \tag{11}$$

where d is the kernel parameter.

Fig. 1 shows the effect of function kernel in different parameter values. RBF kernel has local characteristics and has better learning capability. Moreover, the polynomial kernel function has global characteristics and has strong generalization performance. The performance and complexity of the RUL prediction model of the Li-ion battery are determined by the kernel function.

Smits proposed that improving the performance of SVM using only a single kernel function is difficult [35]. In this paper, an MSVM is proposed to improve the prediction accuracy and generalization capability of SVM. The kernel function of MSVM is composed of the local kernel function K_{RBF} and the global kernel function K_{poly}:

$$K_{new} = \tau K_{RBF} + (1 - \tau)K_{poly} \quad (0 < \tau < 1), \tag{12}$$

where τ is the weight coefficient. The kernel function must satisfy Mercer's theorem, which can be used as the kernel of SVM. The multi-kernel function K_{new}, which is formed by the convex combination of K_{RBF} and K_{poly}, also satisfies the Mercer's theorem.

Fig. 2 shows the effect of the multi-kernel function for the selected test point x = 0.2 in different parameter values τ =0.5, 0.6, 0.7, 0.8, 0.9, among which σ =0.2, d = 2. The multi-kernel function integrates all the characteristics of a traditional single kernel and has improved distribution performance in different datasets.

When τ approaches 0, the polynomial kernel function has a stronger influence on the multi-kernel function, showing the global generalization performance of the polynomial kernel function. When τ approaches 1, the RBF kernel has a greater influence on the multi-kernel kernel function, showing the local fitting performance of the RBF kernel. In the RUL prediction of Li-ion batteries, the weight coefficient τ must be adjusted so that the MSVM is adapted to different data distributions.

III. PARTICLE SWARM OPTIMIZATION ALGORITHM

Section II shows several important parameters in the MSVM model, such as C, σ, d, and τ. The function of the penalty constant C is to find the proper balance between separating error and computational complexity. The characteristics of the training data are reflected by the kernel functions σ and d. The weight coefficient τ is used to assign the weight for K_{RBF} and K_{poly}. All four parameters have direct effects on the performance of the MSVM model. However, for a given problem, it is not known which parameters are optimal in advance. Therefore, the parameters must be optimized before training the MSVM model so that the model can
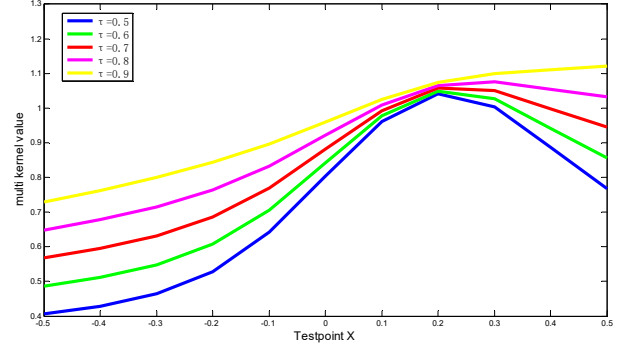

Fig. 2. Test curve of a multi-kernel function.

accurately predict the unknown data.

Grid algorithm is used to optimize the penalty constant C and σ of the RBF in Ref. [36]. However, the feature subset in the grid algorithm cannot be selected at the same time. In Ref. [37], the selection of the feature subset and model parameter for SVM are optimized by GA.

Inspired by the social behavior in nature, PSO, which was proposed by Kennedy and Eberhart [38, 39], is adopted to optimize the parameters of MSVM prediction model in this study.

Similar to other evolutionary algorithms, the PSO algorithm uses a particle swarm to operate. Each particle has two features, namely, its own position and speed, and represents a solution to a problem in the decision space. The current value in the solution is represented by the position, and the direction and distance of the optimal position in the next iteration is defined by velocity.

Each particle changes its search direction based on two factors, namely, its own best previous experience and its best solution in all other members to find the optimal solution [40].

Supposing that n particles formed a population of $X = (X_1, X_2, \dots X_n)$ in M-dimensional space. The M-dimensional position of the particle j at iteration d can be expressed as $x_j^d = \{x_{j1}^d, x_{j2}^d, \dots x_{jM}^d\}$. Likewise, the velocity, which is also an M-dimensional vector, for particle j at iteration d can be expressed as $v_j^d = \{v_{j1}^d, v_{j2}^d, \dots v_{jM}^d\}$. Let $p_j^d = \{p_{j1}^d, p_{j2}^d, \dots p_{jM}^d\}$ be the optimal solution that particle j has obtained until iteration d, and $p_g^d = \{p_{g1}^d, p_{g2}^d, \dots p_{gM}^d\}$ is the optimal solution obtained from p_d^j in the population at iteration d.

In each iteration process, the position and velocity of each particle are updated according to the individual extremum and the global extremum. The updating formula is as follows:

$$V_{jm}^{d+1} = \gamma V_{jm}^d + c_1 r_1 (P_{jm}^d - X_{jm}^d) + c_2 r_2 (P_{gm}^d - X_{jm}^d), \tag{13}$$

and

$$X_{jm}^{d+1} = X_{jm}^d + V_{jm}^{d+1}, \tag{14}$$

where γ is the inertia weight, $m = 1, 2, \dots, M$, d is the current iteration, c_1 and c_2 are constants called acceleration coefficients, r_1 and r_2 are random numbers that follow the uniform distribution (0,1), X_{jm}^d is the previous position and its
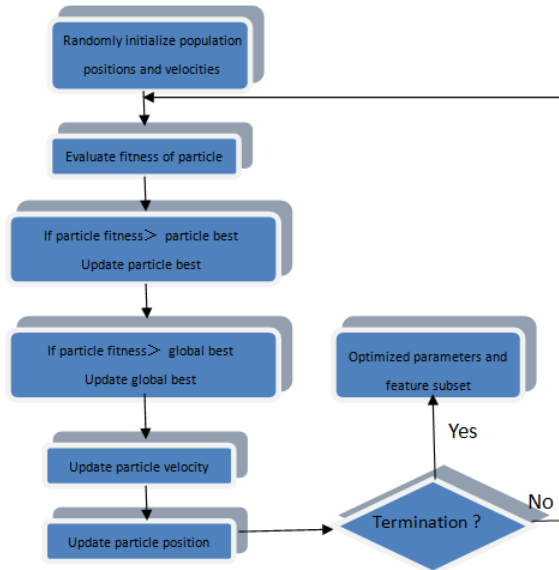
Fig. 3. Flowchart of PSO algorithm.

value   is   limited   within   the   interval $[-X_{max}, X_{max}]$, and V_{jm}^d indicates the previous velocity, which is limited within the interval of $[-V_{max}, V_{max}]$.

The basic process of the PSO algorithm mainly consists of five steps, namely, initialization, fitness evaluate, particle velocity update, construction, and stopping criteria. Each step is defined as follows:

Basic process of PSO algorithm

STEP 1. (Initialization) Randomly initialize the population positions and velocities.

STEP 2. (Evaluate the fitness) Evaluate the fitness of each particle.

STEP 3. (Update particle velocity) Calculate the velocity of each particle in the population according to Formula (13).

STEP 4. (Construction) Calculate the next position of each particle according to the Formula (14).

STEP 5. (Stopping Criteria) If the stopping criterion is satisfied, then stop the PSO algorithm. Otherwise, return to STEP 2.

The iteration ends when the number of iterations reaches the maximum number, which was set in advance.

Fig. 3 shows the computation flowchart for clarity.

IV. PSO–MSVM FOR RUL ESTIMATION OF LI-ION BATTERIES

The principle of the PSO–MSVM algorithm can be obtained based on the aforementioned analysis presented in the flowchart in Fig. 4.

A. Feature Extraction and Selection

The operational parameters that change with the aging of the Li-ion battery should be determined to provide a good
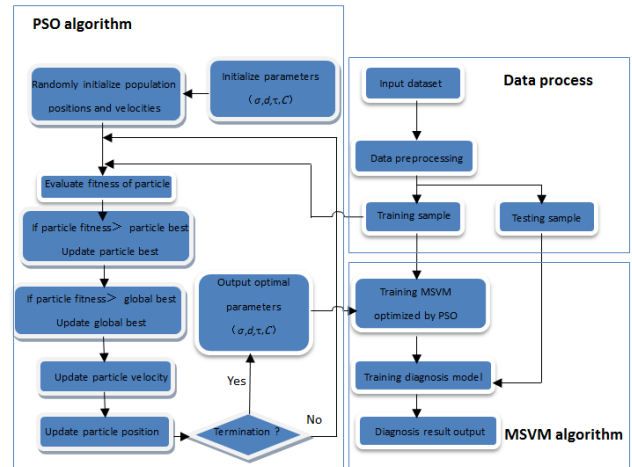

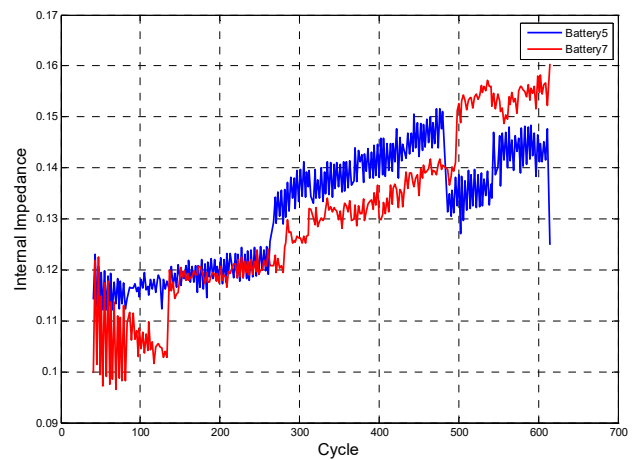Fig. 4. Flowchart of PSO–MSVM algorithm.

Fig. 5. Internal impedance change curve of Nos. 5 and 7 batteries.

indication of the SOH of the Li-ion battery. The accuracy of the SOH estimation and RUL prediction of the Li-ion battery will heavily rely on these features [41]. From the raw data of the Li-ion battery from NASA, a large number of features can be extracted. However, not all of these features are associated with the RUL of Li-ion batteries. To date, several features have been extracted based on three different conditions, namely, charge, discharge, and impedance.

Although the impedance data are accurate, they are difficult to obtain in practical application [35] because the battery must be isolated from the application and electrochemical impedance spectroscopy (EIS) must be employed to measure the AC current. Although the impedance data can be provided by NASA (see Fig. 5), these data are difficult to collect online. Moreover, the measurement of the internal impedance of the Li-ion battery requires a battery model, and the choice of the model directly affects the accuracy of the internal resistance data of the Li-ion battery. The internal impedance measured by the battery model is used to predict the Li-ion battery RUL, which significantly reduces prediction accuracy. Therefore, in this study, the internal impedance cannot be used to predict the RUL of the Li-ion battery.
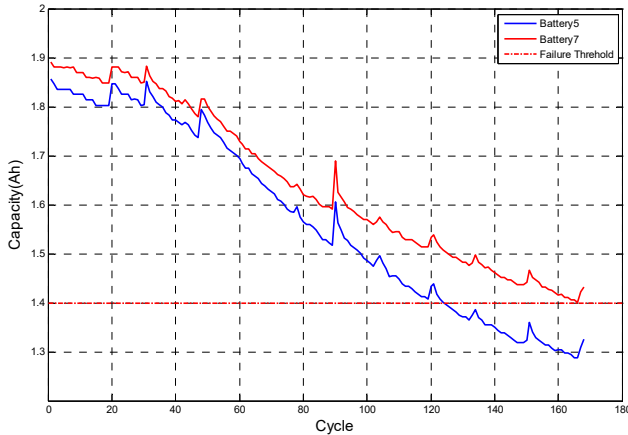
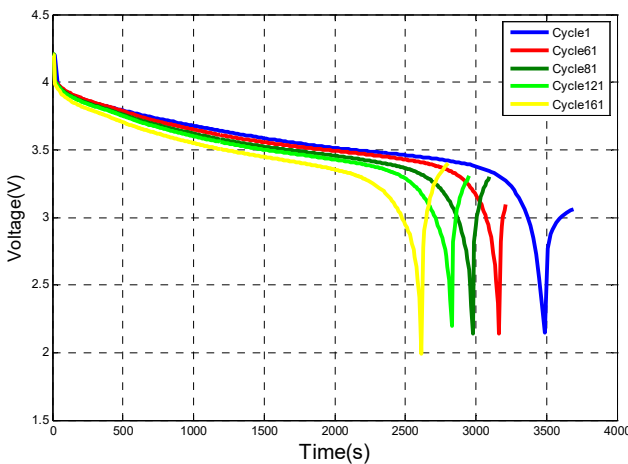Fig. 6. Capacity change curve of Nos. 5 and 7 batteries.

Fig. 7. Voltage curves of different discharge cycles.

Fig. 6 shows that the capacity change curve of Nos. 5 and 7 batteries in discharge cycles are consistent. The Li-ion battery capacity refers to the amount of current that it can supply over time. During the charging and discharging cycles of Li-ion batteries, the capacity decays over time, which is a good way to measure its health. Some spikes are observed in the capacity decay process of Li-ion batteries. These spikes are rest periods of varying lengths in which the capacity appears to increase because the battery test bed has time to be rebalanced [41]. However, these spikes do not affect the RUL prediction of the Li-ion battery because the information of capacity in the use of the process has a very consistent trend. This paper will use capacity as a feature for the RUL estimation of Li-ion batteries.

When the PSO–MSVM algorithm is used to train the Li-ion battery data, the data feature extraction and selection directly affects the accuracy of the prediction. Fig. 7 shows that the discharging voltage curve of each discharge cycle is different. This study selects 500, 1000, 1500, and 2000 s voltage values of each discharge cycle as input data sequence, and the corresponding capacity of each discharge cycle was selected as the output.

B. Li-ion Battery RUL Prediction

The Li-ion battery data used in this study are obtained from the NASA Prognostics Center of Excellence (PCoE) [42], which uses a battery prediction test bench and 18,650 rechargeable batteries sold on the market to collect battery charge and discharge data [43]. The Li-ion batteries operate at room temperature in three different operating conditions, namely, charge, discharge, and full impedance.

Charge mode: Charging was implemented in a constant current mode of 1.5 A until the battery voltage reached 4.2 V, and then maintained a constant voltage mode until the charge current is reduced to 20 mA.

Discharge mode: Discharging was conducted at a constant current level of 2 A until the battery voltage dropped to 2.7 and 2.2 V for battery Nos. 5 and 7, respectively.

Repeated charge and discharge cycles are the main causes of the accelerated fading of a battery. When Li-ion batteries reached up to 30% rated capacity aging (this experiment is from 2 Ah to 1.4 Ah), the experiments were stopped and the Li-ion batteries were considered to have reached their end of life.

Using the NASA Li-ion battery data, this study extracts the data on the discharge cycle to validate our algorithm. The data are divided into two parts, for training and testing the model.

This paper provides the following definitions: RSVM is the SVM algorithm with RBF kernel, PSVM is the SVM algorithm with polynomial kernel, MSVM is the SVM algorithm multi-kernel expressed by Equation (12), and PSO–MSVM is the MSVM optimized by the PSO algorithm.

To verify the superiority of PSO–MSVM, this study is described from the following aspects:

First, this study uses different numbers of training data to train RSVM, PSVM, MSVM, and PSO–MSVM.

Second, this study compares the prediction accuracy of RSVM, PSVM, MSVM, and PSO–MSVM under the same training data.

Fig. 6 shows that the actual end of the lifetime of battery No. 5 is cycle 168, but at this point, the capacity of battery No.7 has not dropped to the failure threshold. Furthermore, this paper focuses on the RUL prediction for the former and the capacity estimation for the latter. RUL prediction and capacity estimation both can verify the predictive ability of these algorithms. Samples 1–80 and 1–112 are selected as the training dataset, and samples 81–168 and 113–168 are used to predict the validation to verify the accuracy of the proposed model for predicting the RUL of Li-ion batteries. When the remaining capacity of the battery reaches the threshold, the end of the battery lifetime is reached.

Figs. 8 and 9 show the RUL prediction of battery No. 5 under different training samples and the predicted results in RSVM, PSVM, MSVM, and PSO–MSVM.

For battery No. 5, this paper defines the following:
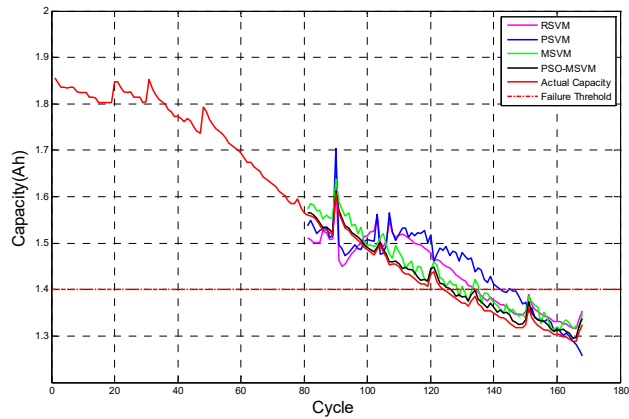
$$AE = |RUL - PRUL|, \tag{15}$$

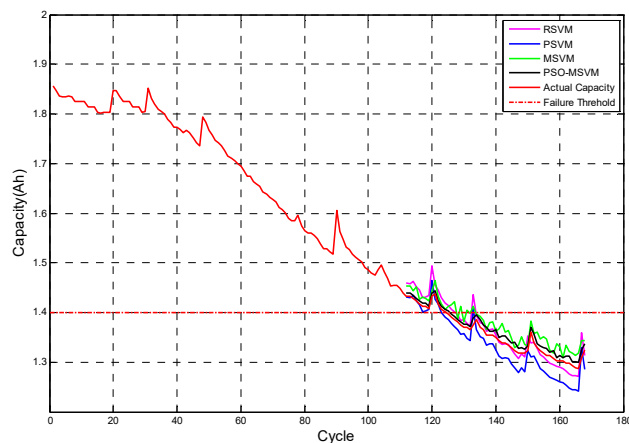Fig. 8. Predicted results in RSVM, PSVM, MSVM, and PSO–MSVM using 80 sets of training data (Battery No. 5).

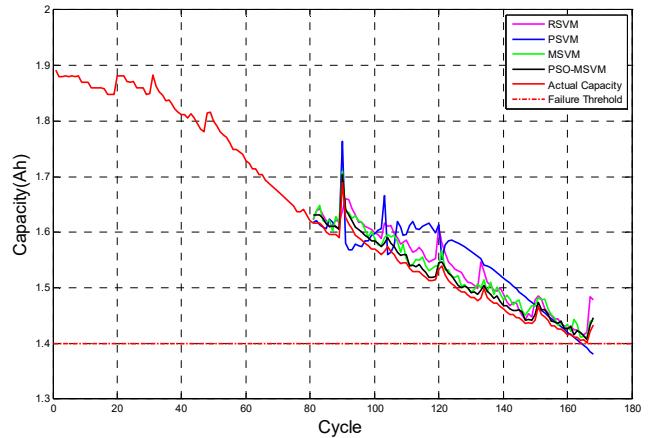Fig. 10. Predicted results of RSVM, PSVM, MSVM, and PSO–MSVM using 80 sets of training data (Battery No. 7).

Fig. 9. Predicted results of RSVM, PSVM, MSVM and PSO–MSVM using 112 sets of training data (Battery No. 5).

Fig 11. Predicted results in RSVM, PSVM, MSVM, and PSO–MSVM using 112 sets of training data (Battery No. 7).

TABLE I

COMPARISON OF CALCULATION RESULTS IN SVM AMONG DIFFERENT KERNEL FUNCTIONS (BATTERY No. 5)

Kernel Function	TS	RUL	PRUL	AE	RE/%
RSVM	80	44	56	12	27.28
	112	12	15	3	25.00
PSVM	80	44	62	18	40.91
	112	12	8	4	33.33
MSVM	80	44	49	5	11.36
	112	12	13	1	8.33
PSO–MSVM	80	44	46	2	4.55
	112	12	12	0	0

and

$$RE = \frac{|RUL - PRUL|}{RUL} \times 100\%, \qquad (16)$$

where RUL is the real RUL value and $PRUL$ is the predicted RUL value, all of which are indexes of prediction performance. TS is the number of training samples. Table I shows the comparison of calculation results in SVM among the different kernel functions.

Figs. 8-9 and Table I show that the RE of PSO–MSVM is smaller than that of RSVM, PSVM, and MSVM with the same TS. For example, with the TS of cycle 80, the RE of PSO–
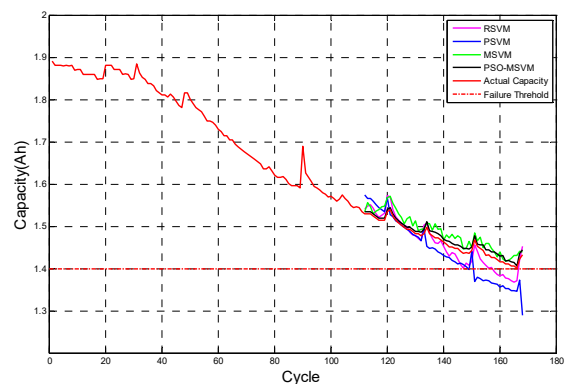
MSVM is 4.55%, whereas the RE of RSVM, PSVM, and MSVM is 27.28%, 40.91%, and 11.36%, respectively. Therefore, PSO–MSVM has better prediction performance in which the errors are all less than 5% with different TS.

Figs. 10 and 11 show the capacity estimation of battery No. 7 under different training samples and the predicted results of RSVM, PSVM, MSVM, and PSO–MSVM.

For battery No. 7, this paper defines the following:

$$MSE = \sqrt{\frac{1}{n}\sum_{i=1}^{n}(y_i - py_i)}, \qquad (17)$$

where y_i is the true capacity value and py_i is the forecast capacity value. TS is the number of training samples. CC is the correlation coefficient. OT is the operating time of the prediction algorithm. Table II shows the comparison of calculation results in SVM among the different kernel functions.

Figs. 10-11 and Table II show that the CC of PSO–MSVM is larger than that of RSVM, PSVM, and MSVM with the same TS. For example, with the TS of cycle 112, the CC of PSO–MSVM is 0.9902, whereas the CC of RSVM, PSVM, and MSVM is 0.9136, 0.8990, and 0.9796, respectively. Moreover, the MSE of PSO–MSVM is smaller than that of RSVM, PSVM, and MSVM with the same TS. For example, with the TS of cycle 80, the MSE of PSO–MSVM is 0.0213,

TABLE II
COMPARISON OF CALCULATION RESULTS IN SVM AMONG
DIFFERENT KERNEL FUNCTIONS (BATTERY NO. 7)

Kernel function	TS	CC	MSE	OT/ms
RSVM	80	0.8921	0.0313	413.16
	112	0.9136	0.0271	503.21
PSVM	80	0.8703	0.0408	475.28
	112	0.8990	0.0395	567.15
MSVM	80	0.9535	0.0263	390.68
	112	0.9796	0.0231	458.54
PSO–MSVM	80	0.9811	0.0213	310.36
	112	0.9902	0.0154	350.25

whereas the CC of RSVM, PSVM, and MSVM is 0.0313, 0.0408, and 0.0263, respectively. Furthermore, the operating time of PSO–MSVM is shorter than that of RSVM, PSVM, and MSVM. Therefore, the RUL prediction and capacity estimation of the Li-ion battery of the PSO–MSVM model is better than that of the other models.

By comparing Figs. 8 and 10 and Figs. 9 and 11, when the RSVM and PSVM are used to predict the RUL of Li-ion batteries using different datasets, all datasets show very poor robustness, whereas MSVM and PSO–MSVM show very good robustness.

In other words, PSO–MSVM has better prediction accuracy and stronger generalization capability, and can reduce the training time and computational complexity.

V. CONCLUSIONS

The main contributions of this study can be summarized as follows:

This paper proposes a PSO–MSVM model to solve the difficulty in predicting the RUL of Li-ion batteries. The advantages of global kernel and local kernel functions are fully considered in this model. An MSVM is constructed using the convex combination of the RBF and polynomial kernels. Moreover, the PSO algorithm is adopted to optimize the parameters of the MSVM model. Subsequently, this paper trains the PSO–MSVM model by using the Li-ion battery data from NASA PCoE. The trained model is used to predict the capacity and RUL of Li-ion batteries. By comparing the aforementioned forecast results among RSVM, PSVM, MSVM, and PSO–MSVM, the proposed method shows better RUL prediction and capacity estimation performance than other traditional single-kernel SVMs in Li-ion batteries.

Compared with conventional single-kernel SVM, the PSO–MSVM model has better prediction accuracy and strong generalization performance in different situations, and its *MSE* is less than 3%. Moreover, the PSO–MSVM model can also reduce training time and computational complexity. The method proposed in this study can provide reliable data for the BMS and other safety systems, and can accurately predict the RUL of Li-ion batteries.

The future work of this study aims to improve the accuracy and efficiency of the PSO–MSVM model. In addition, efforts will be exerted to develop the structure of the kernel function with three kernel functions. Furthermore, experiments will be conducted to collect realistic datasets of the Li-ion battery of EVs, and the realistic datasets will be used to verify the efficiency of the PSO–MSVM model.

REFERENCES

[1] X. Chen, W. Shen, and T. T. Vo, "An overview of lithium-ion batteries for electric vehicles," *IPEC, 2012 Conference on Power & Energy. IEEE*, pp. 230-235, 2012.

[2] Y. Xing, W. M. Ma, and K. L. Tsui, "Battery management systems in electric and hybrid vehicles," *Energies*, Vol. 4, No. 11, pp. 1840-1857, Oct. 2011.

[3] X. S. Si, W. Wang, and C. H. Hu, "Remaining useful life estimation–A review on the statistical data driven approaches," *European Journal of Operational Research*, Vol. 213, No. 1, pp. 1-14, Aug. 2011.

[4] J. C. A. Anton, P. J. G. Nieto, and F. J. D. C. Juez, "Battery state-of-charge estimator using the SVM technique," *Applied Mathematical Modelling*, Vol. 37, No. 9, pp. 6244-6253, May 2013.

[5] V. Klass, M. Behm, and G. Lindbergh, "A support vector machine-based state-of-health estimation method for lithium-ion batteries under electric vehicle operation," *Journal of Power Sources*, Vol. 270, pp. 262-272, Dec. 2014.

[6] M. Galeotti, C. Giammanco, and L. Cinà, "Synthetic methods for the evaluation of the State of Health (SOH) of nickel-metal hydride (NiMH) batteries," *Energy Conversion and Management*, Vol. 92, pp. 1-9, Mar. 2015.

[7] S. Buller, "Impedance-based simulation models for energy storage devices in advanced automotive applications,"[D]. Ph. D. Dissertation, RWTH Aachen, Aachen, Germany, 2003.

[8] G. L. Plett, "Extended Kalman filtering for battery management systems of LiPB-based HEV battery packs: Part 2. Modeling and identification," *Journal of Power Sources*, Vol. 134, No. 2, pp. 262-276, Aug. 2004.

[9] Z. Xu, S. Gao, and S. Yang, "LiFePO4 battery state of charge estimation based on the improved Thevenin equivalent circuit model and Kalman filtering," *Journal of Renewable & Sustainable Energy*, Vol. 8, No. 2, pp. 376-378, Feb. 2016.

[10] K. Goebel, B. Saha, and A. Saxena, "Prognostics in battery health management," *IEEE Instrum. Meas. Mag.*, Vol. 11, No. 4, pp. 33-40, Aug. 2008.

[11] A. Guha, A. Patra, and K. V. Vaisakh, "Remaining useful life

estimation of lithium-ion batteries based on the internal resistance growth model," *Control Conference. IEEE*, pp. 33-38, 2017.

[12] F. Yang, D. Wang, and Y. Xing, "Prognostics of Li(NiMnCo)O$_2$ -based lithium-ion batteries using a novel battery degradation model," *Microelectronics Reliability*, Vol. 70, pp. 70-78, Mar. 2017.

[13] B. Long, W. Xian, and L. Jiang, "An improved autoregressive model by particle swarm optimization for prognostics of lithium-ion batteries," *Microelectronics Reliability*, Vol. 53, No. 6, pp. 821-831, Jun. 2013.

[14] Y. Zhou and M. Huang, "Lithium-ion batteries remaining useful life prediction based on a mixture of empirical mode decomposition and ARIMA model," *Microelectronics Reliability*, Vol. 65, pp. 265-273, Oct. 2016.

[15] X. Zheng and H. Fang, "An integrated unscented Kalman filter and relevance vector regression approach for lithium-ion battery remaining useful life and short-term capacity prediction," *Reliability Engineering & System Safety*, Vol. 144, pp. 74-82, Dec. 2015.

[16] A. Widodo, M. C. Shim, and W. Caesarendra, "Intelligent prognostics for battery health monitoring based on sample entropy," *Expert Systems with Applications*, Vol. 38, No. 9, pp. 11763-11769, Sep. 2011.

[17] E. Walker, S. Rayman, and R. E. White, "Comparison of a particle filter and other state estimation methods for prognostics of lithium-ion batteries," *Journal of Power Sources*, Vol. 287, pp. 1-12, Aug. 2015.

[18] H. Li, D. Pan, and C. L. P. Chen, "Intelligent prognostics for battery health monitoring using the mean entropy and relevance vector machine," *IEEE Trans. Syst., Man, Cybern., Syst.*, Vol. 44, No. 7, pp. 851-862, Jul. 2014.

[19] D. Liu, J. Zhou, and H. Liao, "A health indicator extraction and optimization framework for lithium-ion battery degradation modeling and prognostics," *IEEE Trans. Syst., Man, Cybern., Syst.*, Vol. 45, No. 6, pp. 915-928, Jun. 2015.

[20] M. A. Patil, P. Tagade, and K. S. Hariharan, "A novel multistage Support Vector Machine based approach for Li ion battery remaining useful life estimation," *Applied Energy*, Vol. 159, pp. 285-297, Dec. 2015.

[21] H. Dong, X. Jin, and Y. Lou, "Lithium-ion battery state of health monitoring and remaining useful life prediction based on support vector regression-particle filter," *Journal of Power Sources*, Vol. 271, pp. 114-123, Dec. 2014.

[22] J. Wu, C. Zhang, and Z. Chen, "An online method for lithium-ion battery remaining useful life estimation using importance sampling and neural networks," *Applied Energy*, Vol. 173, pp. 134-140, Jul. 2016.

[23] L. Li, P. Wang, and K. H. Chao, "Remaining Useful Life Prediction for Lithium-Ion Batteries Based on Gaussian Processes Mixture," *Plos One*, Vol. 11, No. 9, pp. e0163004 Sep. 2016.

[24] B. Mo, J. Yu, and D. Tang, "A remaining useful life prediction approach for lithium-ion batteries using Kalman filter and an improved particle filter," *IEEE International Conference on Prognostics and Health Management. IEEE*, pp. 1-5, 2016.

[25] X. Zhang, Q. Miao and Z. Liu, "Remaining useful life prediction of lithium-ion battery using an improved UPF method based on MCMC," *Microelectronics Reliability*, Mar. 2017.

[26] X. Su, S. Wang, and M. Pecht, "Interacting multiple model particle filter for prognostics of lithium-ion batteries," *Microelectronics Reliability*, Vol. 70, pp. 59-69, Mar. 2017.

[27] A. Nuhic, T. Terzimehic, and T. Soczka-Guth, "Health diagnosis and remaining useful life prognostics of lithium-ion batteries using data-driven methods," *Journal of Power Sources*, Vol. 239, pp. 680-688, Oct. 2013.

[28] D. Li, R. M. Mersereau, and S. Simske, "Blind image deconvolution through support vector regression," *IEEE Trans. Neural Netw.*, Vol. 18, No. 3, pp. 931-5, may 2007.

[29] V. Klass, M. Behm, and G. Lindbergh, "A support vector machine-based state-of-health estimation method for lithium-ion batteries under electric vehicle operation," *Journal of Power Sources*, Vol. 270, pp. 262-272, Dec. 2014.

[30] C. Weng, Y. Cui, and J. Sun, "On-board state of health monitoring of lithium-ion batteries using incremental capacity analysis with support vector regression," *Journal of Power Sources*, Vol. 235, pp. 36-44, Aug. 2013.

[31] N. Chen, W. Lu, and J. Yang, "Support Vector Machine," *Machine Learning Models and Algorithms for Big Data Classification. Springer US*, pp.24-52, 2016.

[32] C. Y. Yeh, W. P. Su, and S. J. Lee, "Employing multiple-kernel support vector machines for counterfeit banknote recognition," *Applied Soft Computing*, Vol. 11, No. 1, pp. 1439-1447, Jan. 2011.

[33] M. Gönen and E. Alpaydın, "Cost-conscious multiple kernel learning," *Pattern Recognition Letters*, Vol. 31, No. 9, pp. 959-965, Jul. 2010.

[34] S. Yuan and F. Chu, "Fault diagnosis based on support vector machines with parameter optimisation by artificial immunisation algorithm," *Mechanical Systems and Signal Processing*, Vol. 21, No. 3, pp. 1318-1330, Apr. 2007.

[35] G. F. Smits and E. M. Jordaan, "Improved SVM regression using mixtures of kernels," *International Joint Conference on Neural Networks IEEE Xplore*, pp. 2785-2790, 2002.

[36] C. W. Hsu and C. J. Lin, "A simple decomposition method for support vector machines," *Machine Learning*, Vol. 46, No. 1, pp. 291-314, Jan. 2002.

[37] C. L. Huang and C. J. Wang, "A GA-based feature selection and parameters optimization for support vector machines," *Expert Systems with applications*, Vol. 31, No. 2, pp. 231-240, Aug. 2006.

[38] R. Eberhart and J. Kennedy, "A new optimizer using particle swarm theory," *International Symposium on MICRO Machine and Human Science IEEE*, pp. 39-43, 2002.

[39] J. Kennedy and R. Eberhart, "Particle swarm optimization," *IEEE International Conference on Neural Networks, 1995. Proceedings. IEEE*, pp. 1942-1948, 2002.

[40] S. W. Lin, K. C. Ying, and S. C. Chen, "Particle swarm optimization for parameter determination and feature selection of support vector machines," *Expert systems with applications*, Vol. 35, No. 4, pp. 1817-1824, Nov. 2008.

[41] M. Rezvani, S. Lee, and J. Lee, "A comparative analysis of techniques for electric vehicle battery prognostics and health management (PHM)," *SAE Technical Paper*, Sep. 2011.

[42] B. Saha, K. Goebel, and S. Poll, "Prognostics methods for battery health monitoring using a Bayesian framework," *IEEE Trans. Instrum. Meas.*, Vol. 58, No. 2, pp. 291-296, Feb. 2009.

[43] B. Saha and K. Goebel (2007). "Battery Data Set," NASA Ames Prognostics Data Repository (http://ti.arc.nasa.gov/ project/prognostic-data-repository), NASA Ames Research Center, Moffett Field, CA.

Dong Gao was born in Jiangsu, China in 1992. He received his B.S. degree in Automotive Engineering from Wuhan University of Technology, Wuhan, China, in 2015. He is currently working toward his M.S. degree from the same university. His research interests include electric vehicles, battery management systems, and Li-ion battery SOH estimation and RUL prediction.

Miaohua Huang was born in Jiangxi, China in 1962. She received her B.S. and M.S. degrees in Automotive Engineering from Wuhan University of Technology, Wuhan, China in 1984 and 1990, respectively, and her Ph.D. degree in Mechanical Engineering from Huazhong University of Science and Technology, Wuhan, China, in 2003. She is currently a Professor of Automobile Engineering at Wuhan University of Technology. Her research interests include electric vehicles and on-line fault diagnosis of such vehicles.